Biophysical Chemistry 87 (1987) 87–96
Elsevier

BPC 01159

Dynamic analysis of differential scanning calorimetry data

Obdulio Lopez Mayorga and Ernesto Freire

Department of Biology, The Johns Hopkins University, Baltimore, MD 21218, U.S.A.

Received 16 December 1986
Accepted 9 February 1987

DSC; Dynamic deconvolution; Heat capacity; Kinetics; Ribonuclease A; Dipalmitoylphosphatidylcholine

The apparent heat capacity function measured by high-sensitivity differential scanning calorimetry contains dynamic components of two different origins: (1) an intrinsic component arising from the finite instrument time response; and (2) a sample component arising from the kinetics of the thermal transition under study. The intrinsic instrumental component is always present and its effect on the shape of the experimental curve depends on the magnitude of the calorimeter response time. Usually, high-sensitivity instruments exhibit characteristic time constants varying from 10 to 100 s. This slow response introduces distortions in the shape of the heat capacity function especially at fast scanning rates. In addition to this instrumental component, dynamic effects due to sample relaxation processes also contribute to the shape of the experimental heat capacity profile. Since the nature and magnitude of these effects are a function of the kinetic parameters of the transition, they can be used to obtain kinetic information. This communication presents a dynamic deconvolution technique directed to remove artificial distortions in the shape of the heat capacity function measured at any scanning rate, and to obtain a kinetic characterization of a thermally induced transition. The kinetic characterization obtained by this method allows the researcher to obtain transition relaxation times as a continuous function of temperature. This technique has been applied to the thermal unfolding of ribonuclease A and the pretransition of dipalmitoylphosphatidylcholine (DPPC). In both systems the transition relaxation times are temperature dependent. For the protein system the relaxation time is very slow below the transition temperature (~ 30 s) and very fast above T_m (< 1 s) in agreement with direct kinetic measurements. For the pretransition of DPPC, the relaxation time is maximal at the transition midpoint and of the order of approx. 40 s.

1. Introduction

During the last decade, differential scanning calorimetry has proven to be the single most important technique with which to develop a thermodynamic characterization of temperature-induced conformational and phase transitions in proteins, nucleic acids and biological membranes [1,2]. It has been demonstrated that differential scanning calorimetry is capable not only of providing an accurate measurement of overall thermodynamic parameters like transition enthalpies, entropies and transition temperatures, but also of providing fundamental information concerning the mechanism of temperature-induced transitions [3]. The application of sophisticated deconvolution techniques to the analysis of the heat capacity function associated with macromolecular systems such as multidomain proteins, multisubunit membrane proteins and nucleic acids has permitted the development of precise thermodynamic descriptions of the unfolding mechanism of these complex molecules [4–10].

The resolution of complex heat capacity profiles into individual components as well as the application of statistical thermodynamic methods of analysis require access to an experimentally defined heat capacity function whose shape accurately reflects the equilibrium properties of the process under study. Unfortunately, differential

Correspondence address: E. Freire, Department of Biology, The Johns Hopkins University, Baltimore, MD 21218, U.S.A.

scanning calorimeters introduce distortions in the shape of the heat capacity function as a result of their slow instrumental time response. Typically, high-sensitivity differential scanning calorimeters have intrinsic time responses ranging from approx. 10 to 100 s, thus imposing severe restrictions on the upper scan rate limit that can be used without introducing significant distortions in the heat capacity function. Since the calorimeter sensitivity is directly proportional to the scanning rate it is not possible to reduce arbitrarily the scanning rate in order to obtain distortion free curves. The shape of the measured heat capacity function is also affected by dynamic components arising from the transition kinetics. These effects are more prominent for slow reactions and can be used to obtain kinetic parameters for the transition under study.

The purpose of this communication is two-fold. First, a method to correct instrumental distortions in the shape of the heat capacity function is presented. Second, a dynamic deconvolution procedure directed to obtain kinetic information from dynamically corrected calorimetric data is developed. This method allows determination of relaxation times as a continuous function of temperature from calorimetric scans obtained at different scanning rates. These methods have been applied to the analysis of the gel-liquid crystalline transition of a phospholipid bilayer system and also to the thermal unfolding of ribonuclease A.

2. Materials and methods

The studies reported in this paper were performed with the differential scanning calorimeters Microcal MC1 and Microcal MC2. Both calorimeters have been interfaced to IBM-PC microcomputers using 12 bit analog/digital conversion boards (Data Translation DT-2805 and DT-2801) for automatic data collection. A Privalov DASM1 instrument was available at the University of Granada. For the dynamic characterization of the calorimeters, data were collected at constant time intervals of 0.5 s and scanning rates from 10 to 90 degrees/h were examined. Since the temperature output of these instruments is the jacket and not the cell temperature, the kinetic characterization of the phospholipid and protein transitions were performed with a Microcal MC2 calorimeter especially modified to measure the actual cell temperature.

The phase transition of dipalmitoylphosphatidylcholine (DPPC) bilayers was studied using DPPC fused unilamellar vesicles. DPPC was obtained from Avanti Biochemicals (Birmingham, AL) and its purity checked by thin-layer chromatography. Fused unilamellar vesicles were prepared as described before [10]. Briefly, DPPC, dried under N_2 from a chloroform solution and lyophilized overnight, was suspended and vortex-mixed in 50 mM KCl containing 0.02% NaN_3 at a final concentration of 50 mg/ml. The dispersions were sonicated using a bath sonicator (model G112 SPIG, Laboratory Supplies, Hicksville, NY) and centrifuged at $15\,000 \times g$ for 60 min. During these steps the temperature of the suspension was always maintained above the phospholipid phase transition temperature. The sonicated vesicles were then incubated for 3 weeks at 40 °C. This procedure results in a homogeneous population of large unilamellar vesicles of about 900 Å diameter. For the calorimetric experiments, phospholipid concentrations of 0.1 mg/ml were used. Ribonuclease A from bovine pancreas (type XII-A) was obtained from Sigma Chemical Co. (St. Louis, MO). The experiments described in this communication were performed in 50 mM glycine buffer (pH 3.0) using a protein concentration of 5 mg/ml.

3. Results and discussion

High-sensitivity differential scanning calorimeters are characterized by slow time responses (~ 10–100 s) due primarily to the finite thermal conductivity and heat capacity of the instrument cells, temperature sensors and thermoelectric modules. The characteristics of the distortions introduced by these effects are illustrated in fig. 1 for a typical calorimeter response to a rectangular calibration pulse. Rigorously, the calorimeter response Y^* to an input signal Y can be expressed as the convolution between the input signal and the calorimeter impulse response function, $G(t)$,

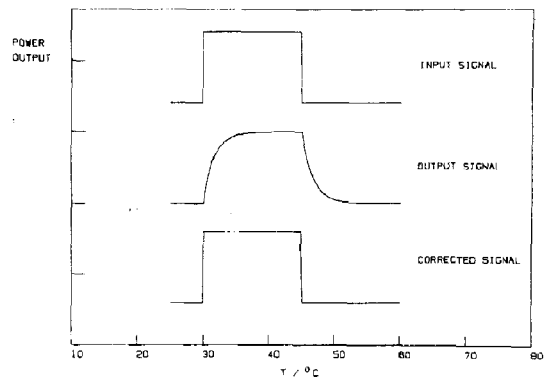

Fig. 1. Typical instrument response (output signal) to a rectangular electrical calibration pulse (input signal). The first task of the dynamic deconvolution method is to remove artificial instrumental distortions in the shape of the signal.

[11]:

$$Y^*(t) = G(t) \otimes Y(t) \tag{1}$$

Mathematically, the Laplace transform of a convolution is equal to the product of the transforms of each individual function, i.e., in the Laplace domain the calorimeter response is equal to the product of the input and transfer functions ($Y(s)G(s)$). For a linear system, the Laplace transform of the first-order impulse response function, $G(s)$, is given by:

$$G(s) = \frac{k}{1 + \tau s} \tag{2}$$

where τ is the characteristic instrumental time constant. $G(s)$ is commonly referred to as the transfer function. After obtaining the inverse Laplace transform, the mathematical relationship between the input and output signal in the time domain becomes:

$$Y(t) = \frac{1}{k}\left(Y^*(t) + \tau \frac{dY^*(t)}{dt} \right) \tag{3}$$

Similarly, for a second-order system eq. 3 becomes:

$$Y(t) = \frac{1}{k}\left[Y^*(t) + (\tau_1 + \tau_2)\frac{dY^*(t)}{dt} + \tau_1\tau_2 \frac{d^2Y^*(t)}{dt^2} \right] \tag{4}$$

In this equation $1/k$ is usually referred to as the calorimeter calibration constant and the τ terms the calorimeter time response constants. Thus, eq. 3 or 4 can be used to correct the experimental calorimetric data and remove instrumental distortions provided that the steady-state calibration constant, the time constants and the time derivative of the experimental data are known.

3.1. Determination of calorimeter time response

The calorimeter time constants can be obtained by fitting the rise or the decay portions of the instrument response to a rectangular electrical calibration pulse to a multiple exponential decay function. For the microcalorimeters available to us for these studies (Microcal MC1, Microcal MC2 and Privalov DASM1) the time response could be satisfactorily described by a single exponential function. Typical time constants for these instruments were approx. 40 and approx. 10 s for the Microcal MC1 and MC2, respectively, and approx. 60 s for the Privalov DASM1 instrument. These three instruments are of the power-compensation type and generally have a much faster time response than instruments of the heat-conduction type [8]. The time constants quoted above represent typical values obtained under normal operation conditions. It must be noted, however, that the actual time constants for these instruments are inversely proportional to the cell feedback voltage used during a particular calorimetric scan. Therefore, applications requiring calorimetric time constants should not rely on typical values but on precisely determined time constants obtained for each calorimetric scan under study.

While the instrument electrical calibration heaters provide a general way of estimating instrumental time constants, it should be noted that in this case the heat path is not identical to that of samples located inside the calorimeter cells. The ability of the calibration heaters to provide accurate dynamic information varies between different instrumental designs and should be evaluated experimentally. This can be done by deconvoluting a very sharp transition using the time constant determined from the analysis of the electrical calibration pulse, and examining the effects of

increasing or decreasing the value of the time constant on the shape of the curve. This concept is illustrated in fig. 2 for the experimentally determined heat capacity function associated with the gel-liquid crystalline transition of DPPC. Fig. 2 shows the experimental curve obtained at 90 degrees/h as well as dynamically corrected curves using time constants of 7, 8.5 and 10 s. As can be observed in this figure, overestimation of the time constant by as little as 15% results in a noticeable overshoot in the decay portion of the deconvoluted curve. Similarly, underestimation of the time constant results in an artificial broadening of the curve.

In order to test the accuracy of the dynamic deconvolution procedure, the same phospholipid sample was scanned at different scanning rates ranging from 10 to 85 degrees/h. The results of these experiments are shown in fig. 3 and indicate that all the dynamically corrected scans are identical within the experimental error. For the six scans shown in fig. 3, the transition temperatures were $41.4 \pm 0.05\,^{\circ}C$, the enthalpies 8.73 ± 0.02 kcal/mol, the peak heights ($C_{p,max}$) 18.06 ± 0.6 kcal/K per mol and the cooperative units ($\Delta H_{vH}/\Delta H$) were equal to 186 ± 6 molecules. These experiments demonstrate that it is possible to recover the correct shape of the heat capacity function from calorimeter scans performed at very fast scanning rates.

3.2. Kinetics of thermally induced transitions

The procedure described above is directed to remove signal distortions introduced by the finite instrumental time response. Once this correction

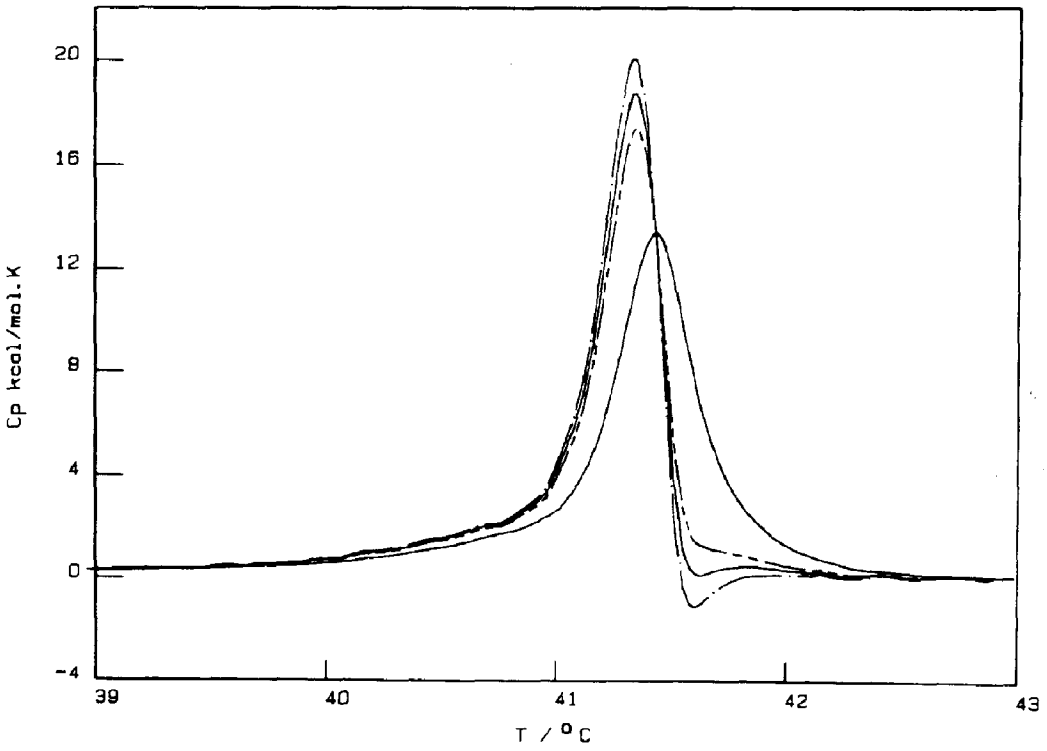

Fig. 2. Dynamic deconvolution of calorimetric data obtained at a scanning rate of 85 degrees/h for the main gel-liquid crystalline transition of DPPC. The broad solid curve represents the raw data and the sharp solid curve the deconvoluted data using the time constant (8.5 s) obtained from the electrical calibration pulse. The additional curves represent data obtained by overestimating (·–·–·) or underestimating (— – — —) the calorimetric time constant by 15%.

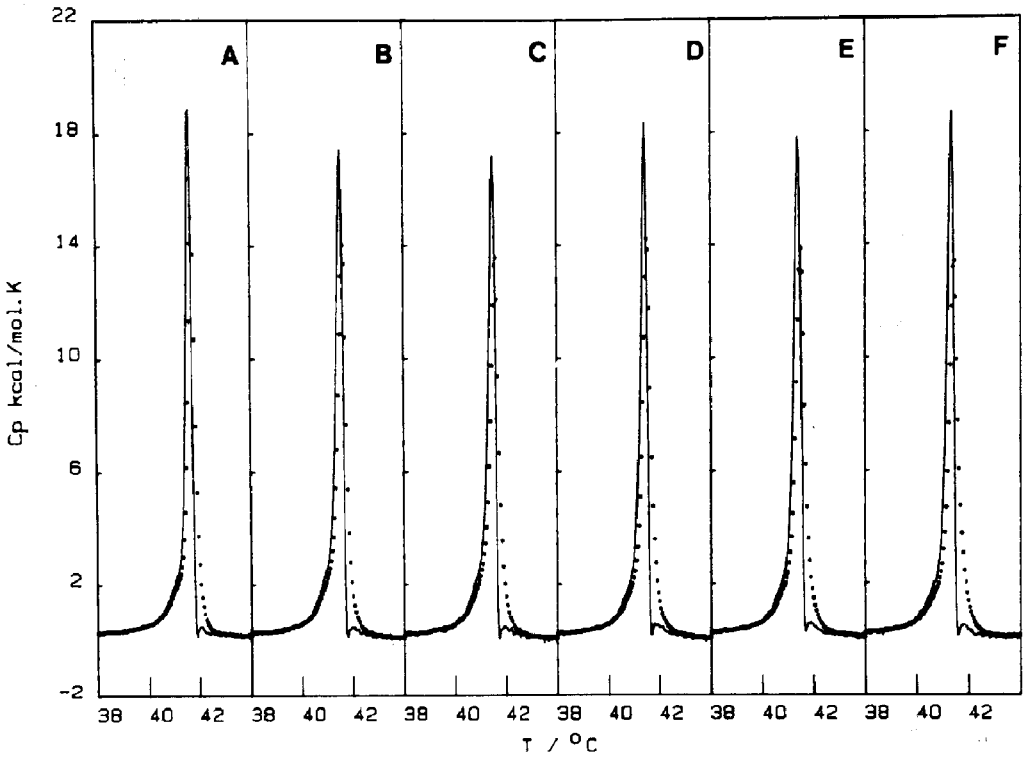

Fig. 3. Dynamically corrected heat capacity function associated with the main gel-liquid crystalline transition of DPPC. The experimental data were obtained at the following scanning rates: (A) 13, (B) 20, (C) 30, (D) 45, (E) 58 and (F) 85 degrees/h, respectively. These curves indicate the efficiency of the deconvolution procedure in removing artificial distortions in the shape of the heat capacity function even at fast scanning rates.

has been done any remaining dynamic components can be attributed to relaxation processes of the sample under study and as such they can be used to estimate kinetic parameters. Using a formalism similar to the one leading to eq. 3 it is possible to express the time-independent, ensemble average value of $\langle \Delta C_p(T) \rangle$ as:

$$\langle \Delta C_p(T) \rangle = \langle \Delta C_p^*(T,\alpha) \rangle + \tau \frac{\partial \langle \Delta C_p^*(T,\alpha) \rangle}{\partial t} \tag{5}$$

Where $\langle \Delta C_p^*(T,\alpha) \rangle$ is the measured value at a scanning rate α and τ the relaxation time for the transition. In this case $\langle \Delta C_p^*(T,\alpha) \rangle$ represents experimental data that have already been corrected for instrumental dynamic distortions as described above.

Since the heat capacity function $\langle \Delta C_p(T) \rangle$ is by definition independent of scanning rate, the right-hand side of eq. 5 must also be independent of scanning rate. Thus, for any two scanning rates the following equation holds:

$$\begin{aligned} \tau &= \frac{\langle \Delta C_p^*(T,\alpha_2) \rangle - \langle \Delta C_p^*(T,\alpha_1) \rangle}{\dfrac{\partial \langle \Delta C_p^*(T,\alpha_1) \rangle}{\partial t} - \dfrac{\partial \langle \Delta C_p^*(T,\alpha_2) \rangle}{\partial t}} \\ &= -\frac{\langle \Delta\Delta C_p^*(T,\alpha_1,\alpha_2) \rangle}{\dfrac{\partial \langle \Delta\Delta C_p^*(T,\alpha_1,\alpha_2) \rangle}{\partial t}} \\ &= -\frac{1}{\dfrac{\partial \ln \langle \Delta\Delta C_p^*(T,\alpha_1,\alpha_2) \rangle}{\partial t}} \end{aligned} \tag{6}$$

and allows determination of the transition relaxation time as a continuous function of temperature from calorimetric scans performed at different scanning rates. It must be noted that eq. 6 is undefined at the points at which the heat capacity profiles obtained at two different scanning rates are numerically equal. Therefore, care must be used when applying eq. 6 to experimental data in order to avoid numerical divergences.

The accuracy of eq. 6 in estimating transition relaxation times was examined by analyzing computer simulated curves generated by assuming different relaxation times and scanning rates for a given set of thermodynamic transition parameters (see the appendix for details). Two examples of this procedure are shown in fig. 4 for a transition characterized by the following overall thermodynamic parameters: $\Delta H = 100$ kcal/mol; $T_m = 55$ and 50 °C; and $\Delta H_{vH}/\Delta H = 1$. The curves in fig. 4 were generated assuming a temperature-independent relaxation time of 30 and 10 s, respectively, and scanning rates of 10 and 90 degrees/h. In general, the observed heat capacity profiles are shifted to higher temperatures at faster scanning rates and the magnitude of the shift is proportional to the transition relaxation time as indicated in fig. 4. Application of eq. 6 correctly yields the relaxation times as shown in the lower panel of the figure. Analysis of computer-simulated curves similar to those shown in fig. 4 indicates that for the range of scanning rates usually accessible to high-sensitivity instruments (~ 10–100

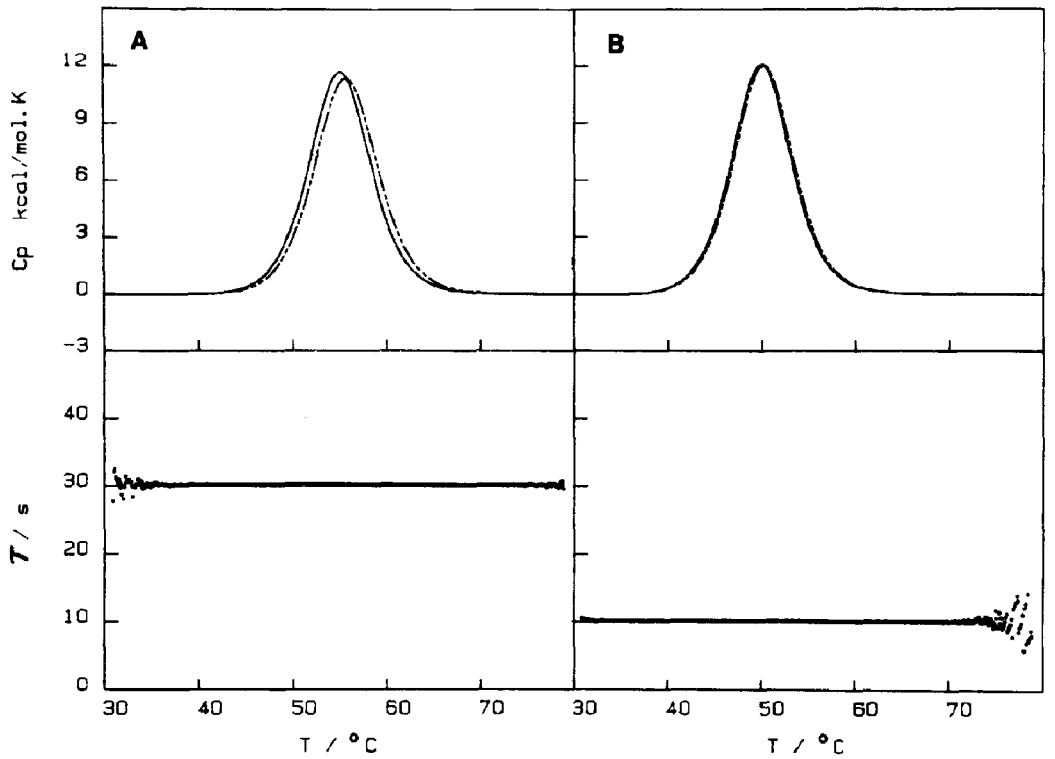

Fig. 4. (Top panels) Computer-simulated calorimetric profiles for a transition characterized by a relaxation time of 30 s (A) and 10 s (B). Solid curves were simulated for a scanning of 10 degrees/h and dotted curves for 90 degrees/h. These curves only contain distortions due to sample relaxation process after removal of all instrumental effects. Thermodynamic parameters for the simulation were $\Delta H = 100$ kcal/mol; $T_m = 55$ °C (A) and 50 °C (B); $\Delta H_{vH}/\Delta H = 1$. (Bottom panels) Relaxation times as a function of temperature calculated from the curves in the top panel using the equations developed in this paper.

degrees/h) relaxation times as fast as 10 s can be determined. For faster transitions, the difference between the curves obtained at the slowest and fastest accessible scanning rates are small compared to uncertainties introduced by baseline determination procedures especially for relatively broad transitions.

3.3. Kinetics of DPPC pretransition

As shown in fig. 3 the dynamic deconvolution of the heat capacity function associated with the main gel-liquid crystalline transition of DPPC results in the complete removal of any scanning rate dependence on the shape of the curves. This type of behavior is the one expected for a transition characterized by a relaxation time faster than the limit of instrumental detectability. In fact, direct kinetic experiments [12] indicate that this transition is characterized by an overall relaxation time faster than 100 ms. Under these conditions, a difference in T_m smaller than 0.01°C is expected between curves obtained at 10 and 90 degrees/h. The situation is different with the phospholipid pretransition centered at approx. 35°C. In this case, removal of the instrumental dynamic distortion does not eliminate the scanning rate dependence of the data. As shown in fig. 5, the transition curves are shifted to higher temperatures at faster scanning rates. This behavior is characteristic for slow transitions and has been observed previously for the pretransition of multilamellar DPPC liposomes [13]. Fig. 6 shows the calculated relaxation time as a function of temperature for the pretransition of DPPC. The three curves in the figure were calculated from separate experiments

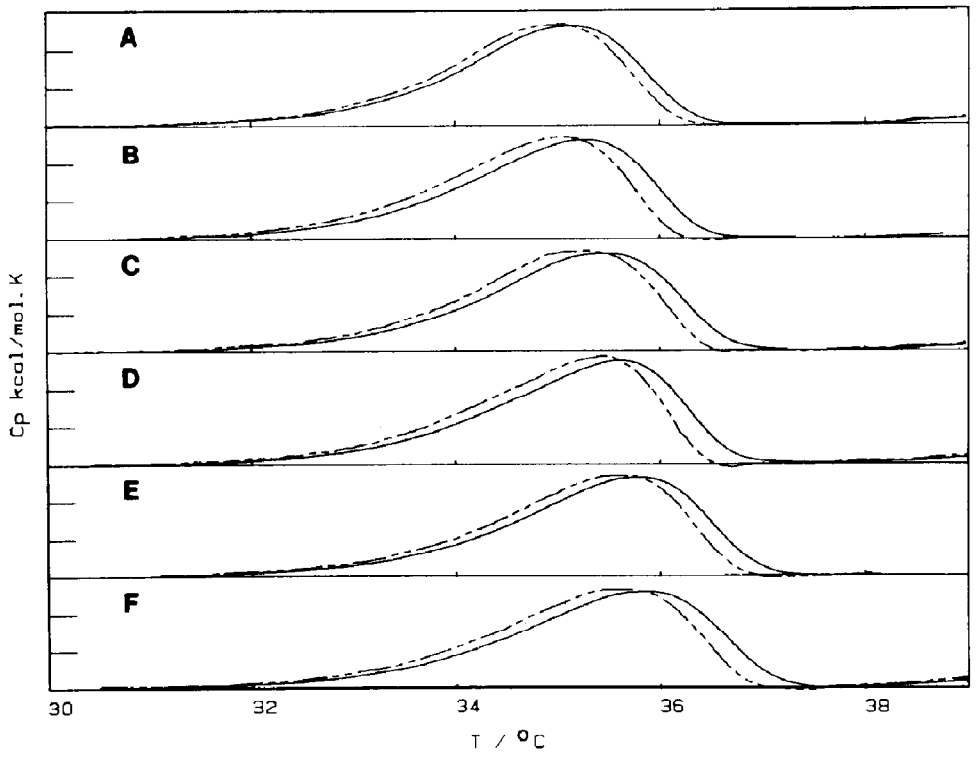

Fig. 5. Calorimetric data (solid curves) and dynamically deconvoluted curves for the pretransition of DPPC. The scanning rates were: (A) 13, (B) 20, (C) 30, (D) 45, (E) 58 and (F) 85 degrees/h, respectively. In this case removal of instrumental distortion does not eliminate the scanning rate variation of calorimetric profile.

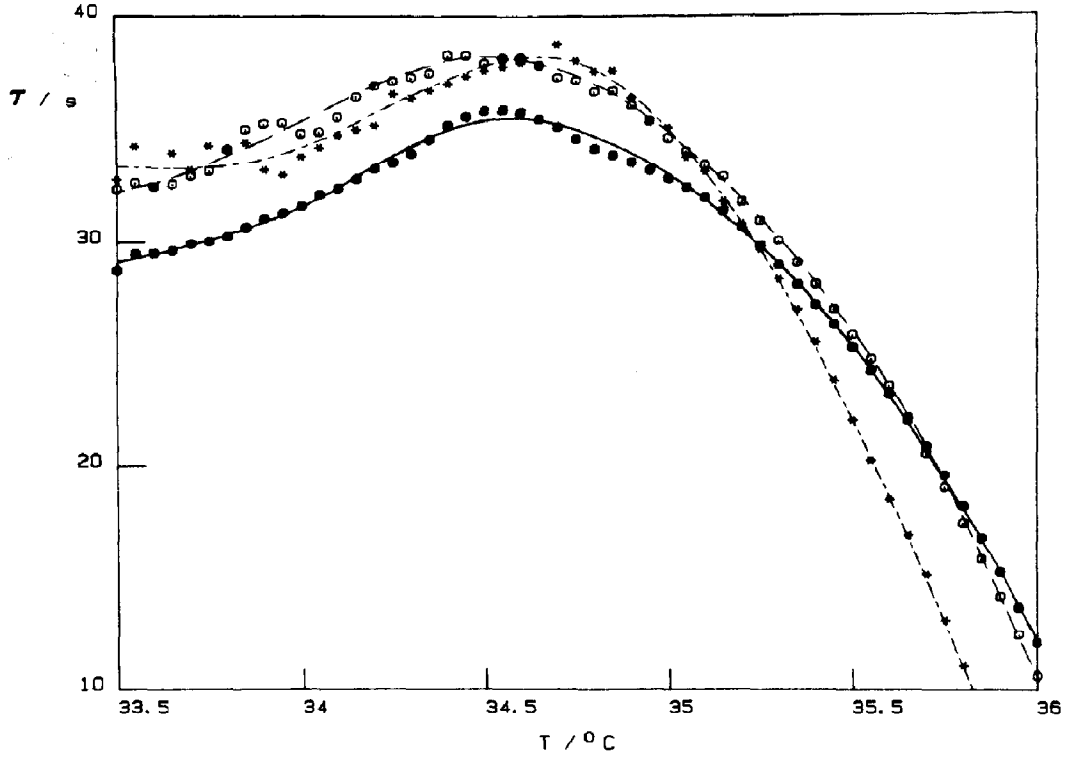

Fig. 6. Relaxation time vs. temperature for the pretransition of DPPC obtained using different scanning rates. (□) 85, (○) 58 and (*) 45 degrees/h. In all cases the reference scanning rate was 13 degrees/h.

performed at three different scanning rate pairs. As shown in the figure, the relaxation time for this transition is strongly dependent on the degree of advancement of the reaction and is maximal at the transition temperature. This type of relaxation time behavior has been observed before for lipid systems [12] and is characteristic of highly cooperative transitions [14].

3.4. Kinetics of the thermal unfolding of ribonuclease A

The kinetics of the folding transition of ribonuclease A has been studied by several authors using stopped-flow and other fast kinetic techniques [15–17]. Experiments performed at temperatures below and above the unfolding transition temperature have revealed that below T_m the kinetics is dominated by the slow phase ($\tau \sim 20$–40 s) and that above T_m the fast phase ($\tau < 1$ s) becomes preponderant. Thus, the relaxation times for this transition are at the limit of the resolution of current instruments. Fig. 7 shows the results obtained by dynamic analysis of differential scanning calorimetry data. In panel A, the experimental curves obtained at 10 and 90 degrees/h are shown. As indicated in the figure, these curves still show a scanning rate dependence after being corrected for instrumental dynamic distortions; in particular, the curve obtained at 90 degrees/h is shifted to higher temperatures. Analysis of the data using eq. 6 yields the transition relaxation time as a function of temperature as depicted in panel B of fig. 7. As shown in this figure, there is a marked increase in the experimental noise level at the point in which the two curves intersect; this is a consequence of the mathematical behavior of eq. 6 as discussed before. In agreement with direct

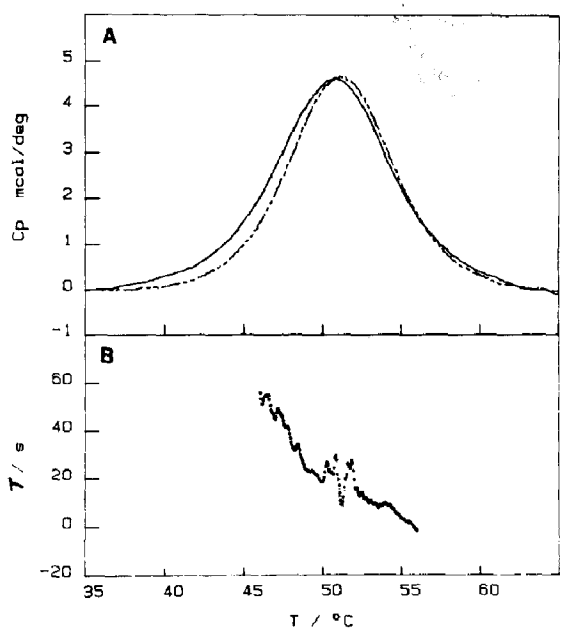

Fig. 7. Calorimetric data associated with the thermal unfolding of ribonuclease A at 10 and 90 degrees/h. The data in panel A have already been dynamically deconvoluted to remove instrumental distortions. Panel B shows the transition relaxation time as a function of temperature calculated from the two curves in panel A as described in the text.

kinetic measurements these data incidate that below T_m the transition is dominated by a slow relaxation time ranging from approx. 50 s at approx. 10 °C below T_m to approx. 10 s immediately below T_m. Above T_m the relaxation time decreases rapidly with temperature until it can no longer be measured with this technique ($\tau < 1$ s). This behavior is similar to that observed using direct kinetic measurements.

4. Conclusions

The studies presented in this paper demonstrate that: (1) it is possible to remove instrumental distortions arising from the finite time response of the calorimeter and obtain correctly shaped heat capacity profiles even at very fast scanning rates; and (2) it is possible to obtain transition relaxation times from dynamically corrected heat capacity curves obtained at different scanning rates. In general, the accuracy with which relaxation times can be calculated is directly proportional to the range of scanning rates available to perform the analysis. With the present generation of high-sensitivity differential scanning calorimeters the maximum attainable scanning rates are of the order of 100 degrees/h. Under these conditions, the fastest relaxation times that can be accurately measured are on the order of 10 s. This lower limit is expected to be improved as faster instruments become available and as high-sensitivity cooling instruments are developed.

Acknowledgements

Supported by grants GM-37911 and NS-24520 from the National Institutes of Health. O.L.M. is on leave from the Department of Physical Chemistry, University of Granada, Spain

Appendix

The dynamically uncorrected apparent heat capacity function associated with a thermally induced transition can be simulated for arbitrary relaxation times, τ, and scanning rates, α, as follows. (1) A continuous temperature scan can be considered as a sequence of infinitely small temperature jumps, ΔT, at time intervals, Δt, determined by the specified scanning rate ($\alpha = \Delta T/\Delta t$). For a small temperature perturbation, the system obeys the linearized rate equations and the excess enthalpy function is given by:

$$\langle \Delta H^*(T_i) \rangle = \langle \Delta H(T_i) \rangle + \left[\langle \Delta H^*(T_i - i) \rangle - \langle \Delta H(T_i) \rangle \right] \exp\left(\frac{-\Delta T}{\alpha \tau} \right) \quad \text{(A1)}$$

where the subscript i corresponds to the i-th elementary temperature step in the transition. $\langle \Delta H(T_i) \rangle$ is the equilibrium value at temperature T_i and $\langle \Delta H^*(T_i - i) \rangle$ the amount of enthalpy absorbed up to the termination of the preceding step. T_0 is the initial temperature. (2) The ob-

served excess heat capacity function is equal to the temperature derivative of the excess enthalpy function $[\langle \Delta C_p^*(T_i) \rangle = \partial \langle \Delta H^*(T_i) \rangle / \partial T)$. (3) Eq. A1 is solved subject to the condition that $\langle \Delta^*(T_0) \rangle$ is equal to its equilibrium value at the initial point of the scan.

References

1 P.L. Privalov and N.N. Khechinashvili, J. Mol. Biol. 86 (1974) 665.
2 R.L. Biltonen and E. Freire, CRC Crit. Rev. Biochem. 5 (1978) 85.
3 E. Freire and R.L. Biltonen, Biopolymers 17 (1978) 463.
4 P.L. Privalov and V.V. Filimonov, J. Mol. Biol. 122 (1978) 447.
5 E. Freire and R.L. Biltonen, Biopolymers 17 (1978) 1257.
6 P.L. Privalov, Adv. Protein Chem. 35 (1982) 1.
7 C.W. Rigell, C. de Saussure and E. Freire, Biochemistry 24 (1985) 5638.
8 J. Suurkuusk, B.R. Lentz, Y. Barenholz, R.L. Biltonen and T.E. Thompson, Biochemistry 15 (1976) 1393.
9 T.N. Tsalkova and P.L. Privalov, J. Mol. Biol. 181 (1985) 533.
10 M. Myers and E. Freire, Biochemistry 24 (1985) 4076.
11 S.L. Randzio and J. Suurkuusk, Biological microcalorimetry, ed. A.E. Beezer (Academic Press, New York, 1980) p. 311.
12 T.Y. Tsong and M. Kanehisa, Biochemistry 16 (1977) 2674.
13 B.R. Lentz, E. Freire and R.L. Biltonen, Biochemistry 17 (1978) 4475.
14 G. Schwarz, J. Mol. Biol. 11 (1965) 64.
15 T.Y. Tsong, R.L. Baldwin and P.L. McPhie, J. Mol. Biol. 63 (1972) 453.
16 P.J. Hagerman and R.L. Baldwin, Biochemistry 15 (1976) 1462.
17 L.N. Lin and J.F. Brandts, Biochemistry 22 (1983) 573.